

# Interaction of human trophoblast cells with gland-like endometrial spheroids: a model system for trophoblast invasion

V.U. Buck, B. Gellersen, R.E. Leube, and I. Classen-Linke\*

Institute of Molecular and Cellular Anatomy, Medical Faculty, RWTH Aachen University, Wendlingweg 2, 52074 Aachen, Germany

\*Correspondence address. Tel: +49-241-80-88-924; Fax: +49-241-80-82-50-8; E-mail: iclassen-linke@ukaachen.de;  
URL: <http://www.ukaachen.de/kliniken-institute/institut-fuer-molekulare-und-zellulaere-anatomie.html>

Submitted on August 27, 2014; resubmitted on December 2, 2014; accepted on January 12, 2015

**STUDY QUESTION:** Do maternal endometrial epithelial cell (EEC) differentiation and polarity impact the invasive capacity of extravillous trophoblast (EVT) cells during early human implantation?

**SUMMARY ANSWER:** In a three dimensional (3D) confrontation co-culture the invasiveness of the human trophoblast cell line AC-1M88 was inversely correlated with the degree of differentiation and polarization of human endometrial adenocarcinoma cell spheroids.

**WHAT IS KNOWN ALREADY:** In a previous study desmosomal and adherens junction proteins were shown to spread from a subapically restricted lateral position to the entire lateral membrane in human glandular EECs during the implantation window of the menstrual cycle. Whether this change in EEC junction localization has an impact on the interaction of EVT cells with glandular EECs during early human implantation is not known.

**STUDY DESIGN, SIZE, DURATION:** A new 3D cell culture system was developed in order to mimic early implantation events in humans. As a model for the invasion of endometrial glands by EVT cells, spheroids of three differently differentiated and polarized endometrial adenocarcinoma cell lines were confronted with an EVT cell line in co-culture experiments.

**PARTICIPANTS/MATERIALS, SETTING, METHODS:** Three human adenocarcinoma EEC lines were chosen for this study because of their differences in differentiation and polarization: HEC-1-A, which is well differentiated and highly polarized, Ishikawa, which is well differentiated and moderately polarized, and RL95-2, which is moderately differentiated and poorly polarized. When the cell lines were grown in reconstituted basement membrane, they formed gland-like, multicellular spheroids. The degree of polarization within the different EEC spheroids was assessed by 3D confocal immunofluorescence microscopy detecting the basal membrane protein integrin  $\alpha 6$ , the apical tight junction-associated protein ZO-1 and the desmosomal plaque protein desmoplakin 1/2 (Dsp). Cells of the human EVT cell line AC-1M88, which is a fusion cell line of primary EVT cells and choriocarcinoma-derived JEG-3 cells, were added to the different EEC spheroids to examine their interaction. For the analyses of trophoblast-endometrial confrontation sites, HLA-G was used as a specific EVT cell marker.

**MAIN RESULTS AND THE ROLE OF CHANCE:** The endometrial HEC-1-A and Ishikawa cells formed gland-like structures in reconstituted basement membrane with apicobasal polarization towards their well-developed internal lumina, while most of the RL95-2 spheroids showed no lumen formation at all. The three EEC lines strongly differed in their apicobasal distribution pattern of Dsp. Ishikawa and HEC-1-A spheroids showed a subapical concentration of Dsp. In contrast, an equal distribution of Dsp was discerned along the entire lateral membranes in RL95-2 spheroids. In 3D confrontation co-cultures the highest invasiveness of AC-1M88 was observed in the poorly polarized RL95-2 spheroids.

**LIMITATIONS, REASONS FOR CAUTION:** Human endometrial and trophoblast cell lines were used for this study because of ethical and legal restrictions for implantation studies with human blastocysts and because of limited access to primary human endometrial cells.

**WIDER IMPLICATIONS OF THE FINDINGS:** The presented 3D cell culture system can be used to investigate the contribution of epithelial junctions to trophoblast-endometrial interactions. The identified impact of endometrial differentiation and polarity on the invasiveness of EVT cells improves our understanding of the relevance of endometrial receptivity for early implantation and may contribute to higher success rates in assisted reproductive technology.

**STUDY FUNDING/COMPETING INTEREST(S):** This work was supported by Grant I46/14, 'START-Program', Medical Faculty, RWTH Aachen University, to V.U.B., by Grant Lec\_I6\_12, 'RWTH Lecturer Award', RWTH Aachen University to I.C.-L. and by the German Research Council (Grant LE 566-20-1). The authors declare no conflict of interest.

**Key words:** endometrial epithelial cells / trophoblast / human implantation / three dimensional cell culture / epithelial junctions

## Introduction

Implantation of the embryo into the endometrium marks the onset of placentation and is a prerequisite for survival of the conceptus and a successful pregnancy. According to clinical data obtained from IVF studies, pregnancy rates are low (30–35%). The major reasons for this low efficiency are neither fully understood nor completely identified (Koot et al., 2012). The quality of implanting embryos is probably one of the reasons. In addition, the differentiation of the endometrium to a state of receptivity is most likely another essential prerequisite for successful implantation. Early implantation in humans is accompanied by adhesion to and invasion of the endometrial epithelium. Based on studies of early primate implantation sites an intrusive implantation mode has been proposed for humans (Enders, 2000). This mode differs considerably from implantation modes of other mammalian species including animals commonly used for laboratory experiments such as mice, rats and rabbits (Schlafke and Enders, 1975). According to the comprehensive image collection of Allen C. Enders (<http://www.trophoblast.cam.ac.uk/info/enders.shtml>; 24 January 2015, date last accessed) there are even slight differences between early human and primate implantation, especially with respect to the invasiveness of the trophoblast. Because of this unique situation the use of animal models for examining trophoblast invasion during early implantation is limited. In addition, because of ethical constraints, the *in vivo* investigation of early human implantation is not possible. Therefore, there is an urgent need for suitable *in vitro* models to examine early implantation. One of the rare *ex vivo* studies using human surplus IVF embryos revealed that trophoblast cells open junctional complexes between endometrial epithelial cells (EEC) to penetrate the epithelial cell layer (Bentin-Ley et al., 2000). This study further indicated that the observed intrusive implantation mode is accompanied by the formation of junctional contacts, especially desmosomes, between trophoblast cells and EECs. We have shown previously that desmosomes and adherens junctions of human glandular EECs are redistributed from a subapical position to the entire lateral plasma membrane during the implantation window of the menstrual cycle (Buck et al., 2012). We proposed that these changes prepare the endometrial epithelium for implantation. Based on these findings the aim of the present study was to develop an *in vitro* co-culture system which would help to establish whether the altered distribution of maternal epithelial junctions influences the penetration and invasion of trophoblast cells. Previous *in vitro* models for human implantation used trophoblast cell lines grown as multicellular spheroids to mimic the spherical structure of the blastocyst during the early attachment phase and early invasion into the endometrium (Grummer et al., 1994; Thie et al., 1998; Hohn and Denker, 2002; Thie and Denker, 2002; Gonzalez et al., 2011; Lee et al., 2011; Holmberg et al., 2012; Wang et al., 2012, 2013; Gellersen et al., 2013; Schmitz et al., 2014). Such spheroids mimicking the trophectodermal layer of the blastocyst were confronted with human EECs and endometrial stromal cells, which were grown as

simple monolayers. These experiments therefore mainly focused on the attachment and outgrowth of the trophoblast multicellular spheroids on the recipient cells and not on the invasive process itself. In contrast to these previous approaches, we now investigate invasion of extravillous trophoblast (EVT) cells into and through intact endometrial gland-like spheroids which occurs after apposition and adhesion of the blastocyst. The new combined EVT-EEC *in vitro* model described here will help to further elucidate endometrial receptivity and the involvement of epithelial junctions during early implantation.

## Materials and Methods

### Cell lines

Three endometrial adenocarcinoma cell lines were used in co-culture experiments with the trophoblast cell line AC-IM88. The HEC-1-A cell line (HTB-112) and the RL95-2 cell line (CRL-1671) were purchased from the American Type Culture Collection (ATCC, Manassas, VA, USA). The Ishikawa cell line (99040201) was purchased from the European Collection of Cell Cultures (ECACC, Salisbury, UK). The hybridoma cell line, AC-IM88, a fusion of primary EVT cells and the JEG-3 choriocarcinoma cell line, was kindly provided by H.G. Frank and P. Kaufmann (University Hospital Aachen, Germany) (Funayama et al., 1997; Gaus et al., 1997). The endometrial cell lines were cultured according to the suppliers' recommendations. HEC-1-A were kept in phenol red-free McCoy's 5a Medium (Hyclone, South Logan, UT, USA) supplemented with PSF 100× (100 U/ml penicillin, 100 µg/ml streptomycin, 25 µg/ml Fungizone®; PAA, Pasching, Austria) and 10% charcoal-stripped fetal calf serum (cs-FCS; C.C.Pro, Oberdorla, Germany). Ishikawa cells were cultured in phenol red-free minimum essential medium (Gibco, Paisley, UK) supplemented with PSF 100×, 2 mM L-glutamine (Gibco), 1% non-essential amino acids (100×; PAA) and 5% cs-FCS. RL95-2 cells were cultured in phenol red-free Dulbecco's modified Eagle's medium (DMEM)/F12 Medium (C.C.Pro) supplemented with PSF 100×, 2.5 mM L-glutamine (Gibco), 5 µg/ml human recombinant insulin (Gibco), and 10% cs-FCS. AC-IM88 cells have been described previously and were propagated as published (Gellersen et al., 2010). They were cultured in phenol red-free DMEM/F12 Medium (C.C.Pro) supplemented with 2.5 mM L-glutamine (Gibco), 100 U/ml penicillin, 100 µg/ml streptomycin (both from PAA, Pasching, Austria) and 10% cs-FCS. All cell lines were kept in an incubator at 37°C in a humid atmosphere with 5% CO<sub>2</sub>. Media were changed every second day.

### Combined culture of EEC spheroids and monolayers

Subconfluent monolayers of EECs in cell culture plastic dishes were washed with phosphate-buffered saline (PBS, without Ca<sup>2+</sup> and Mg<sup>2+</sup>) for 10 min at 37°C and 5% CO<sub>2</sub>. After incubation in PBS containing 0.25% (w/v) trypsin (BD, Sparks, MD, USA) and 0.02% (w/v) EDTA (Sigma-Aldrich, Steinheim, Germany) for 2 min, the remaining cell clusters were dissociated into single cell suspensions by aspiration into a 1000 µl pipet tip for 20 times. The single cell suspensions were centrifuged at 106 × g for 5 min, resuspended

in serum-free medium and then cooled on ice for 15 min. The single cell suspensions were then mixed with an equal volume of ice-cold, phenol red-free Matrigel™ (BD Biosciences, Bedford, MA, USA/Cat. No. 356237) to a final concentration of  $5 \times 10^5$  cells/ml. Twenty microlitre droplets of the Matrigel™-cell suspensions were then plated individually into the centre of LabTek™ 8-well glass slide chambers (Nalge Nunc, Rochester, NY, USA) and allowed to solidify for 30 min (Fig. 1a). Then 500  $\mu$ l cell culture medium containing  $1 \times 10^4$  single cells of the same cell line was added to each chamber and the cells spread onto the Matrigel™-cell droplets and on the glass substrate around them (Fig. 1b and c).

### Confrontation of EEC monolayers and spheroids with trophoblast cells

At Day 4 of the combined two dimensional (2D) and three dimensional (3D) EEC cultures, trophoblast AC-1M88 cells were added. To this end, subconfluent AC-1M88 monolayers were trypsinized and dissociated into single cell suspensions as described above. The EEC medium was then removed from the LabTek™-chambers and replaced by 500  $\mu$ l AC-1M88 culture medium containing  $1 \times 10^3$  single AC-1M88 cells per well (Fig. 1d). After 5 more days (Fig. 1e) the cultures were fixed and subjected to immunofluorescence staining for simultaneous analyses of single EEC spheroids and trophoblast-endometrial confrontation sites in 2D and 3D (Fig. 1f).

### Immunofluorescence

Detailed information on all antibodies and controls is provided in Table 1. Cell culture medium was removed and the LabTek™-chambers were washed with PBS at 37°C for 5 min. The cells were then fixed in methanol for 5 min at  $-20^\circ\text{C}$ , air dried for 15 min and rehydrated in PBS for 10 min at room temperature. Antibodies were diluted in PBS supplemented with 1.5% bovine serum albumin. After incubation of cells with primary antibodies for 48 h at 4°C the chambers were washed with PBS three times for 40 min at room temperature. Incubation with secondary antibodies was performed for 24 h in the dark at 4°C. For nuclear staining 1  $\mu$ g/ml 40,6-diamidino-2-

phenylindole, dihydrochloride (DAPI; Sigma, Hamburg, Germany) was added to the secondary antibody solution and incubated for 30 min at room temperature. Chambers were again washed with PBS ( $3 \times$  for 40 min at RT). The stained cultures were then rinsed briefly in deionised water. After removing the LabTek™-chambers the slides were mounted with Kaiser's glycerol gelatin (Merck, Darmstadt, Germany) and stored at 4°C until microscopic assessment. For double labelling both primary antibodies were applied simultaneously. Similarly, both secondary antibodies were mixed in the next incubation step. For controls, the specific primary antibodies were either omitted or replaced by IgG isotypes and non-immune sera, as listed in Table 1. No specific staining of these negative controls was observed (Supplementary Fig. S1).

### Experimental setup and microscopic analysis

Cell culture experiments were performed in three different assays, independently. Each experiment for the particular spheroids of the different cell lines was performed in duplicate. The total number of trophoblast-endometrial confrontation sites was counted in one experiment to be 135 for HEC-1-A cells, 129 for Ishikawa cells and 121 for RL95-2 cells. The average number of trophoblast-endometrial confrontation sites per well (8-well LabTek™-slide) in the 3D matrix was 16.88 (SEM 3.31) for HEC-1-A cells, 16.13 (SEM 4.05) for Ishikawa cells and 15.13 (SEM 2.36) for RL95-2 cells.

Immunofluorescence staining was assessed by confocal laser scanning microscopy using a LSM 710 Duo (Zeiss, Jena, Germany). Epifluorescence and differential interference contrast (DIC) images were also recorded by an Axio Imager M.2 microscope with an ApoTome.2 unit using an AxioCam MRm camera. Pictures were evaluated using the Zeiss ZEN 2009 software and the AxioVision software (version 4.8; Zeiss, Jena, Germany). Image processing and 3D projections of exported z-stack slices were performed using the ImageJ-based image processing program Fiji. In total, 170 confocal 3D scans were performed: 32 z-stack scans of single HEC-1-A cell spheroids, 44 scans of single Ishikawa spheroids, 25 scans of single RL95-2 spheroids, 19 scans of trophoblast-endometrial confrontation sites for HEC-1-A cells, 32 for Ishikawa cells and 18 for RL95-2 cells.

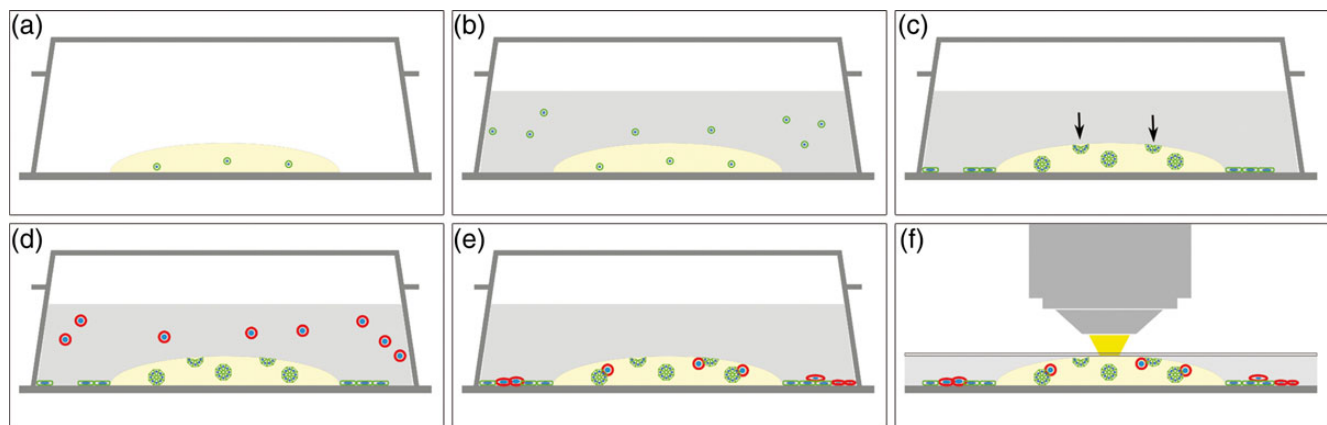


**Figure 1** Mixed 2D/3D culture of human endometrial epithelial cell (EEC) lines and confrontation with human AC-1M88 trophoblast cells. (a) Single EECs (green) were mixed with liquid Matrigel™ and plated as droplets into the centre of LabTek™ 8-well slide chambers. (b) After gelling, medium containing single cells of the same EEC line was added. (c) During 4 days in culture the cells inside the gels proliferated and formed multicellular spheroids. The EECs plated after solidification of the gels also formed multicellular structures at the surface of the gels (arrows). Cells formed monolayers on the glass around the gel droplets. (d) At Day 4 a single cell suspension of AC-1M88 trophoblast cells (red) was added on top of the mixed 2D/3D cultures. (e) After a 5 further days in culture the AC-1M88 trophoblast cells had invaded the Matrigel™ and attached to EEC spheroids as well as to the monolayers around the gel. (f) The co-cultures were fixed and immunofluorescence staining was performed on the slides. Morphology of gland-like spheroids and the trophoblast-endometrial confrontation sites were assessed by confocal microscopy.

**Table 1** List of antibodies and sera used in the study of interactions between human trophoblast cells and gland-like endometrial spheroids.

	Antigen/serum/ conjugate	Host (isotype)	Clone (Cat. No.)	Source	Dilution
Primary antibodies	Integrin $\alpha 6$	Rat (IgG2a)	GoH3	BD Pharmingen, Bedford, MA, USA	1:200
	Desmoplakin 1/2	Guinea pig polyclonal	DP 495	Progen Biotechnik, Heidelberg, Germany	1:500
	ZO-1	Rabbit polyclonal	(# 40-2200)	Invitrogen, Carmarilla, CA, USA	1:200
	HLA-G	Mouse (IgG1)	4H84	Antibodies-online, Aachen, Germany	1:5000
Controls	Rat isotype control	(IgG2a)	(# 16-4321_81)	ebioscience, San Diego, CA, USA	[according to primary antibodies]
	Normal guinea pig serum		(# 006-000-001)	Jackson/Dianova, West Grove, USA	
	Non-immune rabbit IgG	(IgG)	(# NIR-1G)	Enzyme Research, South Bend, IN, USA	
Secondary antibodies	Mouse negative control	(IgG1)	(# X0931)	DAKO, Glostrup, Denmark	
	Alexa Fluor 555 anti rat	Goat (IgG H+L)	(# A-21434)	Invitrogen, Eugene, USA	1:500
	Alexa Fluor 488 anti guinea pig	goat (IgG H+L)	(# A-11073)	Invitrogen, Eugene, USA	1:500
	Alexa Fluor 555 anti guinea pig	goat (IgG H+L)	(# A-21435)	Invitrogen, Eugene, USA	1:500
	Cy3 anti rabbit	donkey (IgG H+L) F(ab') <sub>2</sub>	(# 711-166-152)	Jackson, West Grove, USA	1:500
	Alexa Fluor 488 anti mouse	goat (IgG H+L) F(ab') <sub>2</sub>	(# A-11029)	Invitrogen, Eugene, USA	1:500

## Results

### Establishment of a combined 2D and 3D culture system

In order to generate EEC-derived gland-like structures in a 3D Matrigel™ system for trophoblast invasion assays, appropriate culture conditions had to be determined. The densities of cells within and on top of the gels turned out to be critical for this purpose. Also, the duration of trypsinization and of mechanical dissociation had to be adjusted for every cell line. Under optimized conditions EECs spontaneously formed multicellular structures of similar size inside the Matrigel™-matrix. EECs plated on top of thick gels also formed multicellular spheroids that grew into and on top of the Matrigel™. To obtain combined 2D/3D cell cultures in one well, single droplets of Matrigel™ with embedded trypsinized EECs were placed into the centre of each LabTek™-chamber and a single cell suspension of EECs was added after 4 days for formation of a monolayer next to the gel-associated spheroids (Fig. 1c).

### Lumen formation and distribution of desmosomes in endometrial epithelial spheroids

The morphology of HEC-1-A, Ishikawa and RL95-2 spheroids was assessed by phase contrast microscopy and was further characterized by confocal fluorescence microscopy of whole-mount immunofluorescence stainings after 9 days of culture. Structures were classified as

spheroids only when they were round and consisted of a single layered epithelium with basally localized nuclei (Figs 2 and 3). Spheroids of all three cell lines were positive for the basal membrane marker integrin  $\alpha 6$ , which localized in each instance to the basal margin of the EECs as determined by DIC microscopy (Fig. 2). Lumen formation was assessed by staining the tight junction protein ZO-1. HEC-1-A and Ishikawa spheroids showed distinct ZO-1 staining surrounding lumina in cross sections (Figs 2, 3c and g). In contrast, RL95-2 spheroids did not develop a regularly shaped lumen. A dot-like ZO-1 staining was found only occasionally inside RL95-2 spheroids (Fig. 2k). The distribution of desmosomes was examined by staining the desmosomal plaque protein desmoplakin 1/2 (Dsp) (Fig. 3b, f and j). In HEC-1-A spheroids Dsp was concentrated towards the central lumen. The density of desmosomal dots decreased considerably towards the basal margin of the lateral membranes (Fig. 3b). In Ishikawa spheroids Dsp-positive dots were also concentrated close to the internal lumina. However, the rest of the lateral plasma membranes showed no gradual reduction of desmosomes towards the basal margins but an equal distribution of desmosomes, albeit at a lower density than in the immediate subapical domain (Fig. 3f). In RL95-2 spheroids the dot-like Dsp staining was equally distributed along the lateral plasma membranes without any apical enrichment (Fig. 3j).

### Desmosomal contacts between EECs and AC-1M88 trophoblast cells in 2D

Trophoblast-endometrial confrontation was achieved by addition of single AC-1M88 trophoblast cells on top of the gels that contained the

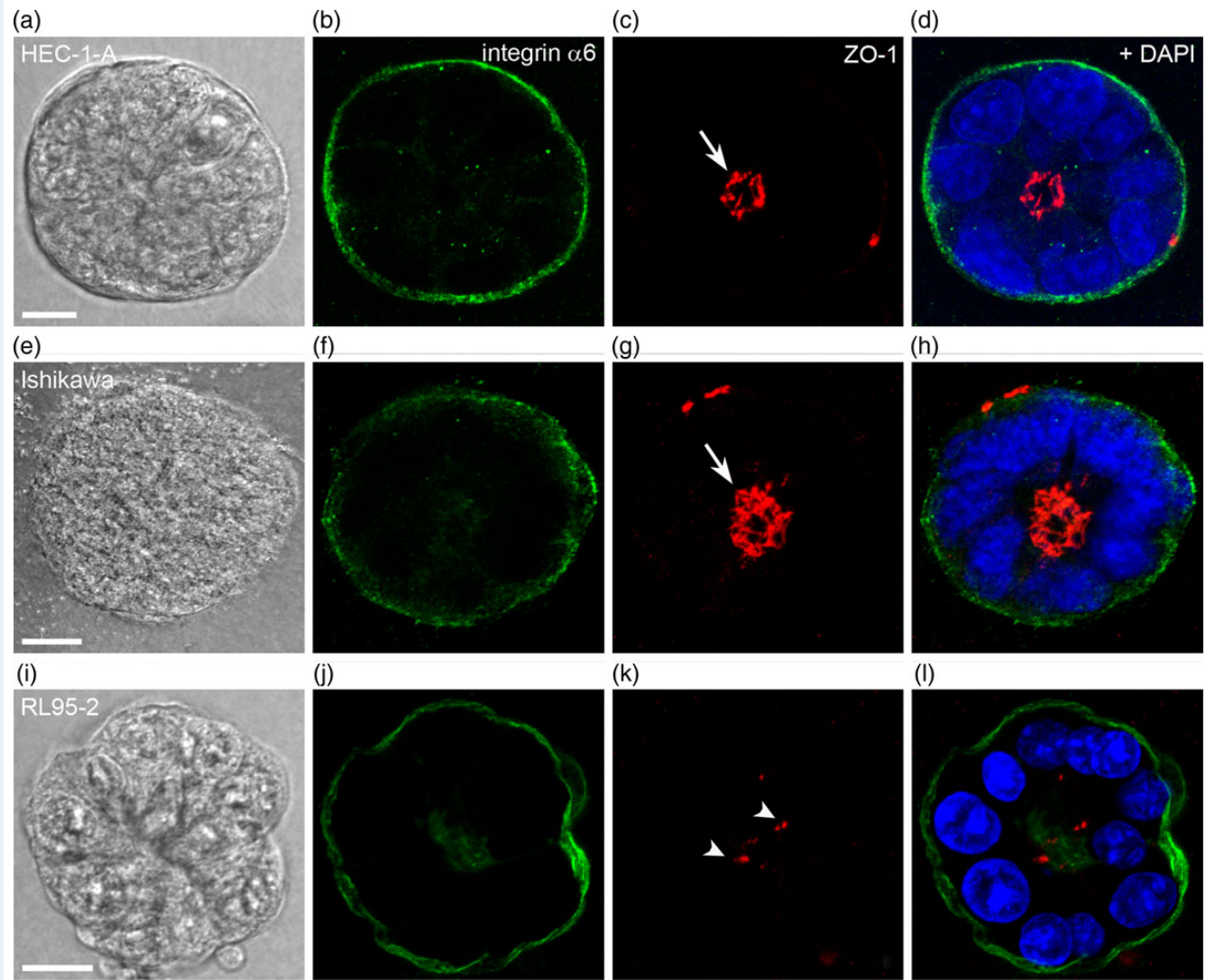


**Figure 2** Morphology and lumen formation of human EEC lines in three dimensional (3D) culture. Spheroids of the three different EEC lines after 9 days in Matrigel™ are shown. Immunofluorescence staining was performed to detect integrin  $\alpha 6$  and ZO-1. Z-projections of five consecutive confocal planes through the middle of standard spheroids are presented. Standard spheroids consisted of a single epithelial cell layer with basal localization of the 4',6-Diamidino-2-phenylindole (DAPI) stained nuclei (blue; **d**, **h** and **l**). At the basal margin of the spheroids towards the surrounding gel, which was visualized by differential interference contrast (DIC/**a**, **e** and **i**), all three cell lines showed a positive integrin  $\alpha 6$  staining (green; **b**, **f** and **j**). In HEC-1-A and Ishikawa spheroids, distinct lumina surrounded by ZO-1 staining (red; arrows in **c** and **g**) were formed. In RL95-2 spheroids lumen formation was not detected. Dot-like ZO-1 staining occurred only in the centre of some spheroids (arrowheads in **k**). Scale bars represent 10  $\mu\text{m}$  and apply to all images in the row.

pre-cultured EEC spheroids and to the EEC monolayers next to them on the glass slide. 2D confrontation sites were assessed in regions where AC-IM88 cells encountered the EECs in the x-y-plane. Distinct contacts could be identified between the different cell types by Dsp staining at the cell borders (Fig. 4c, g and k). In contrast to the exclusive punctate Dsp staining at the plasma membrane of EECs, the trophoblast cells showed additional staining of filamentous structures in the cytoplasm. While the trophoblast cells were found in between RL95-2 and Ishikawa monolayers (Fig. 4h and l), they stayed separated from HEC-1-A monolayers (Fig. 4d).

### Invasiveness of AC-IM88 trophoblast cells into 3D spheroids differs between the three recipient EEC lines

When single AC-IM88 cells were placed on top of the pre-cultured EEC spheroids, they subsequently invaded the Matrigel™-matrix and were found attached to EEC spheroids after 5 days of co-culture (Fig. 5). The invasive capacity of AC-IM88 trophoblast cells differed in these 3D confrontation approaches depending on the grade of differentiation of the investigated EEC line. Cell line HEC-1-A, with the strongest

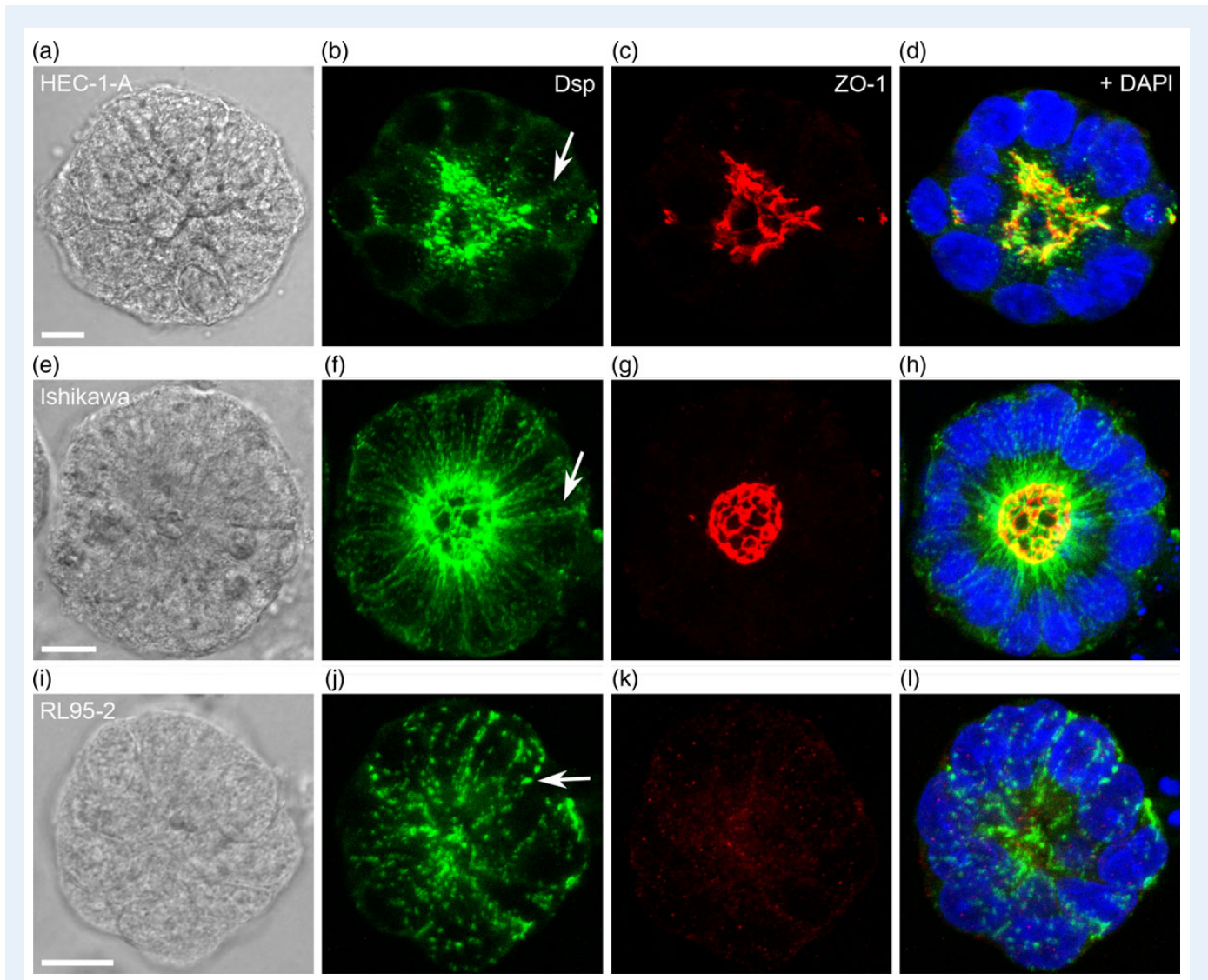


**Figure 3** Distribution of desmosomes correlates with the proposed polarity of human EEC lines. Spheroids of the three different EEC lines after 9 days in Matrigel™ are shown. Immunofluorescence staining was performed to detect desmoplakin 1/2 (Dsp) and ZO-1. Z-projections of eight consecutive confocal planes through the middle of standard spheroids are presented. DIC micrographs are shown in **a**, **e** and **i**. Fluorescence pictures were merged and combined with nuclear staining (DAPI, blue) in **d**, **h** and **l**. Arrows in **b**, **f** and **j** depict lateral plasma membranes of adjacent epithelial cells. In HEC-1-A spheroids dot-like staining of the desmosomal plaque protein Dsp (green) was concentrated in the subapical regions of lateral plasma membranes. Towards the basal margins of lateral membranes the desmosomal dots were strongly decreased in number (**b**). Ishikawa spheroids also showed a subapical concentration of desmosomes. The density of desmosomal dots was lower at the total lateral membranes than in the subapical region. In contrast to HEC-1-A spheroids, however, there was no decrease of desmosomes towards the basal margins (**f**). Both HEC-1-A and Ishikawa spheroids formed lumina surrounded by the tight junctional protein ZO-1 (red stain; **c** and **g**). In RL95-2 spheroids lumen formation was not detected (**k**). The desmosomes of RL95-2 spheroids cells were equally distributed along the entire lateral plasma membranes and showed no concentration towards the centre of the spheroids (**j**). Scale bars represent 10  $\mu\text{m}$  and apply to all images in the row.

polarization of gland-like spheroids (Figs 2 and 3), was not invaded by AC-IM88 trophoblast cells. The trophoblast cells were only attached to the HEC-1-A spheroids (Fig. 5a–d). The large lumina of HEC-1-A spheroids often had an elongated shape. When those lumina were not in the centre of the spheroids but closer to one side, the AC-IM88 cells attached to the other side of the highly polarized spheroids in all investigated sites. At confrontation sites with Ishikawa cell spheroids, the AC-IM88 trophoblast cells displayed a more invasive phenotype with distinct cell protrusions compared with confrontation sites with

HEC-1-A spheroids. The trophoblast cells not only attached to the Ishikawa spheroids but also penetrated the EEC spheroid by forming long protrusions (Fig. 5e–h). Again, AC-IM88 cells were attached to apparently less polarized regions of the Ishikawa spheroids. As expected, the poorly polarized RL95-2 spheroids were even more efficiently penetrated by AC-IM88 trophoblast cells. The trophoblast cells not only intruded into the endometrial epithelial spheroids with cellular protrusions (Fig. 5i and j) but also their entire somata were found in between the RL95-2 cells (Fig. 5l). In 3D projections of the confrontation sites

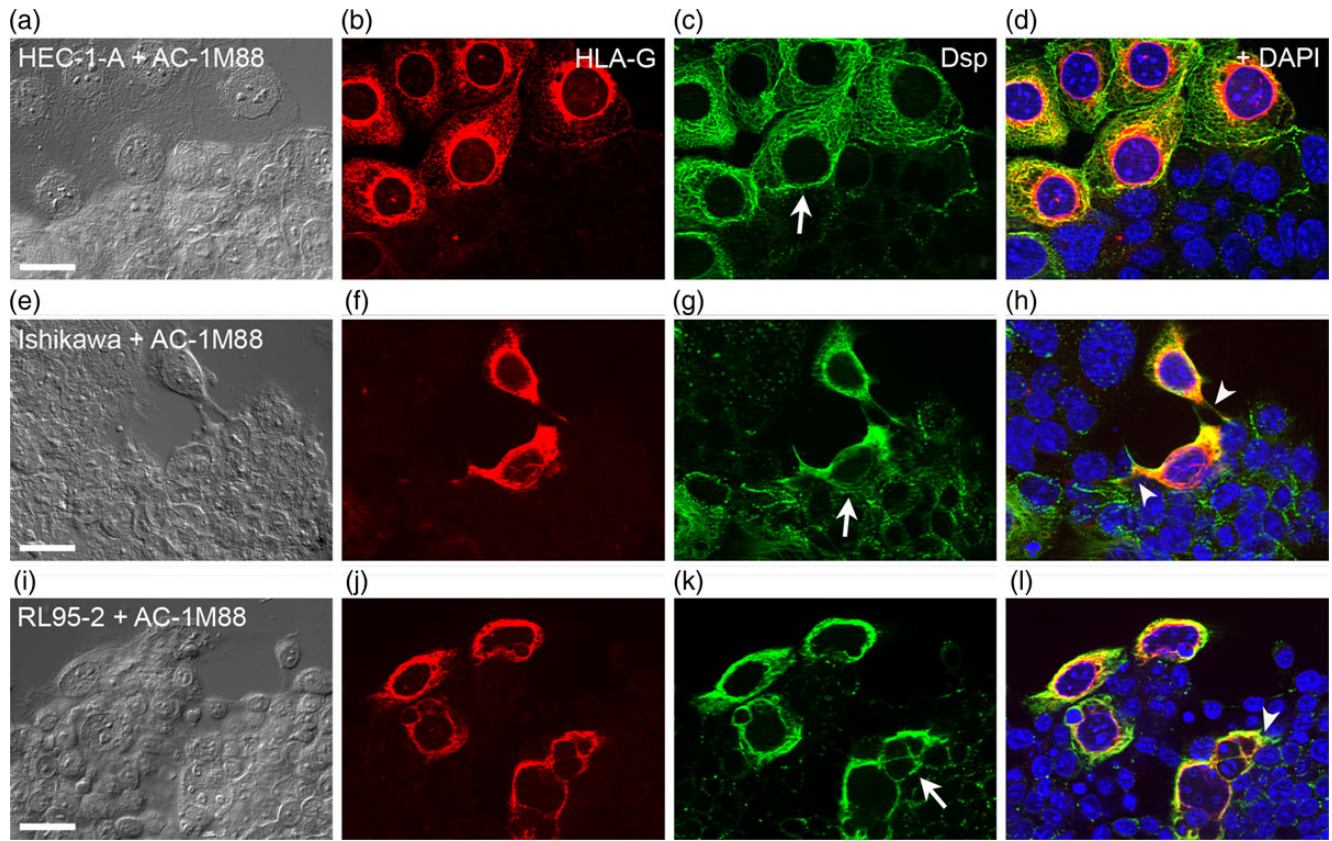


**Figure 4** Human trophoblast-endometrial interaction in monolayer confrontation culture (2D). Confrontation sites of EEC line monolayers with AC-1M88 trophoblast cells after 9 days in culture and 5 days after addition of trophoblast cells are depicted. Immunofluorescence staining was performed to localize Dsp (green stain) and HLA-G, which specifically stains EVT cells (red). DIC pictures in **a**, **e** and **i**. Epifluorescence micrographs were merged and combined with nuclear staining (DAPI, blue) in **d**, **h** and **l**. Pictures were taken from peripheral regions of LabTek™-wells where EEC monolayers on glass were not confluent. AC-1M88 cells were found in between gaps of EEC monolayers and approached EECs in x-y direction. While HEC-1-A cell monolayers were just attached to AC-1M88 cells (**a–d**), the trophoblast cells were found in between RL95-2 and Ishikawa monolayers (**e–l**). Distinct Dsp-positive dots were found at the cell borders between the trophoblast cells and EECs (arrows in **c**, **g** and **k**). In addition, cellular protrusions of AC-1M88 cells towards and into Ishikawa and RL95-2 cell monolayers were observed (arrowheads in **h** and **l**). Scale bars represent 10  $\mu$ m and apply to all images in the row.

the interspersed trophoblast cells had a stretched, elongated shape (Fig. 6b). At the tip of those extensive cellular protrusions desmosomal contacts to the surrounding EECs could be detected (Fig. 6d). Furthermore, when confrontation sites with very large RL95-2 spheroids were analysed, single AC-1M88 cells were found to be completely integrated into the EEC cluster (Fig. 6e–h). This situation was only seen at confrontation sites of AC-1M88 cells with RL95-2 spheroids and not at those with spheroids of the more differentiated and stronger polarized EEC lines HEC-1-A and Ishikawa.

## Discussion

Our new combined 2D and 3D cell culture model provides useful information on aspects of trophoblast invasion and the role of EECs during early implantation of human embryos and first trimester placentation. The three endometrial cancer cell lines that we examined are well established epithelial cell lines that have been used in several studies (Way *et al.*, 1983; Kuramoto *et al.*, 2002; Nishida, 2002). They were

chosen on the basis of their morphology and polarity that had been described in various *in vitro* implantation models (Hannan *et al.*, 2010). Observations obtained in these implantation models have so far indicated that the polarity of EECs is inversely related to the adhesiveness of trophoblast spheroids to their surface. In terms of EEC invasion and penetration, however, these observations are only of limited relevance because they focused on the attachment of trophoblast spheroids to the apical surface of EECs (Grummer *et al.*, 1994; Thie *et al.*, 1996, 1998; Thie and Denker, 2002; Holmberg *et al.*, 2012).

Here we present a culture system which additionally allows the study of later phases of the embryonic implantation and invasion process including the invasion of trophoblast cells into glandular structures. This is possible because we inverted the co-culture arrangement by preparing endometrium-derived and not trophoblast-derived spheroids. This situation mimics the morphology of endometrial glands and therefore reflects the invasion process from the basement membrane. The unique arrangement of our cell culture setup facilitates, in addition, the simultaneous monitoring of confrontation in two and three dimensions.

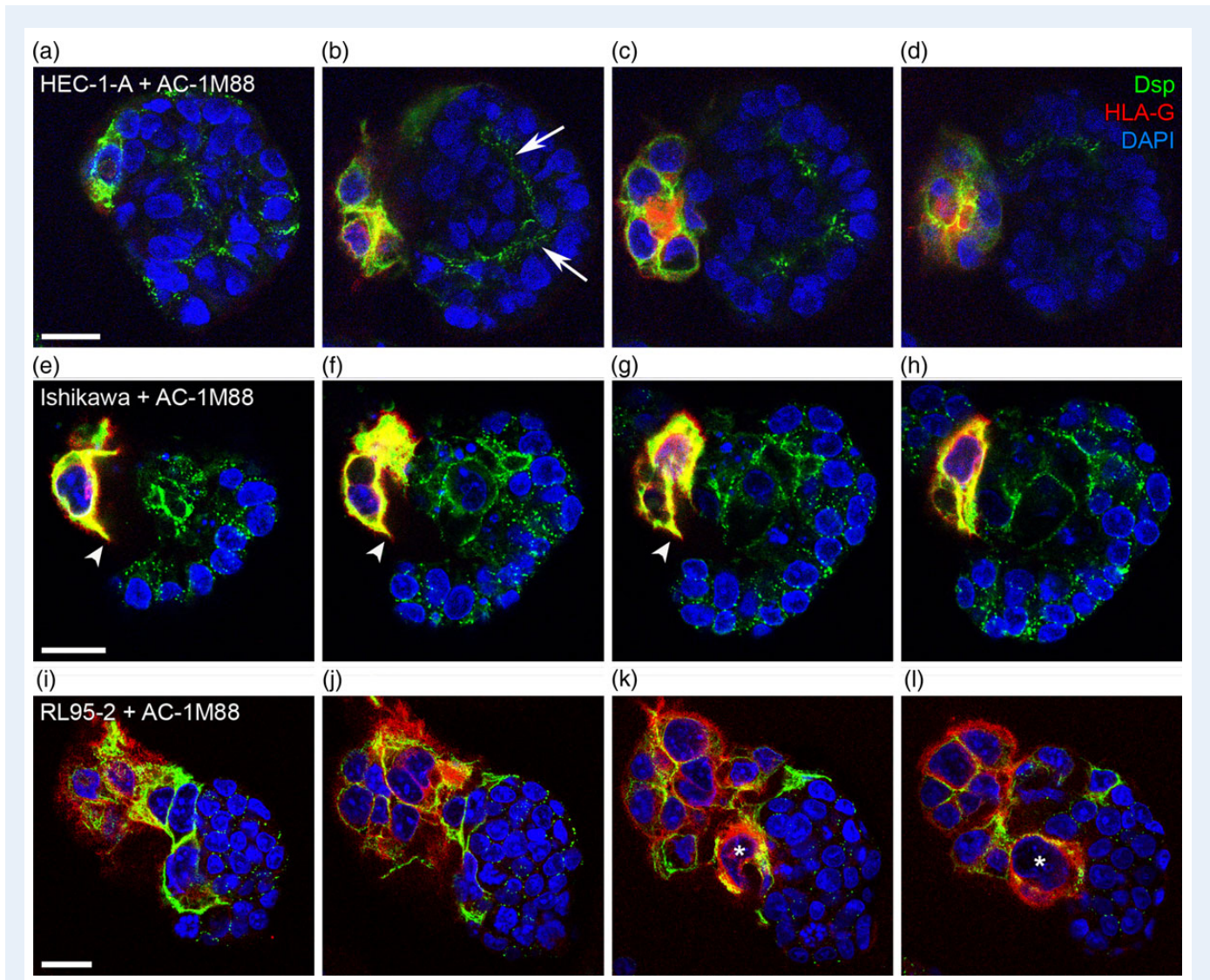


**Figure 5** Human trophoblast-endometrial interaction inside the Matrigel<sup>TM</sup>-matrix (3D). Confrontation sites of EEC spheroids with AC-1M88 trophoblast cells after 9 days in Matrigel<sup>TM</sup> and 5 days after addition of trophoblast cells are shown. Immunofluorescence staining was performed to detect Dsp (green) and HLA-G (red), which specifically stains EVT cells, and was combined with DAPI (blue) for nuclear staining. Four consecutive confocal planes of a z-stack scan are shown from left to right for each EEC line. The trophoblast cell line AC-1M88 revealed a more intrusive and invasive phenotype when co-cultured with a less polarized and less differentiated EEC line in the 3D environment. AC-1M88 cells were found to be barely attached to the highly polarized HEC-1-A cell spheroids. Attachment sites were often found most distant to the large, sometimes tubular lumina, which were only found in HEC-1A spheroids (arrows in **b**). At confrontation sites with Ishikawa spheroids the AC-1M88 cells grew into the EEC spheroids with cellular protrusions (arrowheads in **e–g**). RL95-2 spheroids were strongly invaded by the trophoblast cells that were found integrated into the EEC clusters in confocal cross sections (asterisks in **k–l**). Scale bars represent 20  $\mu\text{m}$  and apply to all images in the row.

By combining 2D and 3D cultures in the same assay it became possible to directly compare the invasion of trophoblast cells between EEC cells in the x-y-plane with the more complex invasion into 3D spheroids in the gel matrix. Trophoblast cells invaded RL95-2 and Ishikawa cell monolayers, but stayed separated from the strongly polarized HEC-1-A monolayer. In case of the 3D cell culture, the trophoblast cells barely attached to the HEC-1-A spheroids but invaded Ishikawa and RL95-2 spheroids to a different extent as determined in confocal cross sections.

The previously observed changes in glandular EEC junction distribution and polarity coinciding with the implantation window of the menstrual cycle (Buck et al., 2012) are most likely induced by changes in ovarian

steroid hormone levels. The differently polarized EEC lines used in the current study mimic these physiologically occurring changes in EEC polarity. The strongly polarized phenotype of HEC-1-A cells in the 3D culture—in terms of the distribution of junction markers—is similar to that observed in EECs from proliferative endometrial tissue samples. Conversely, the junction distribution of the poorly polarized RL95-2 cells correlates to the EEC junction distribution of the secretory endometrial samples during the implantation window (Buck et al., 2012). So far, changes in desmosomal distribution in EECs during implantation have been primarily investigated in animal models (Illingworth et al., 2000; Preston et al., 2006). There is only one report on human surplus IVF blastocysts that were



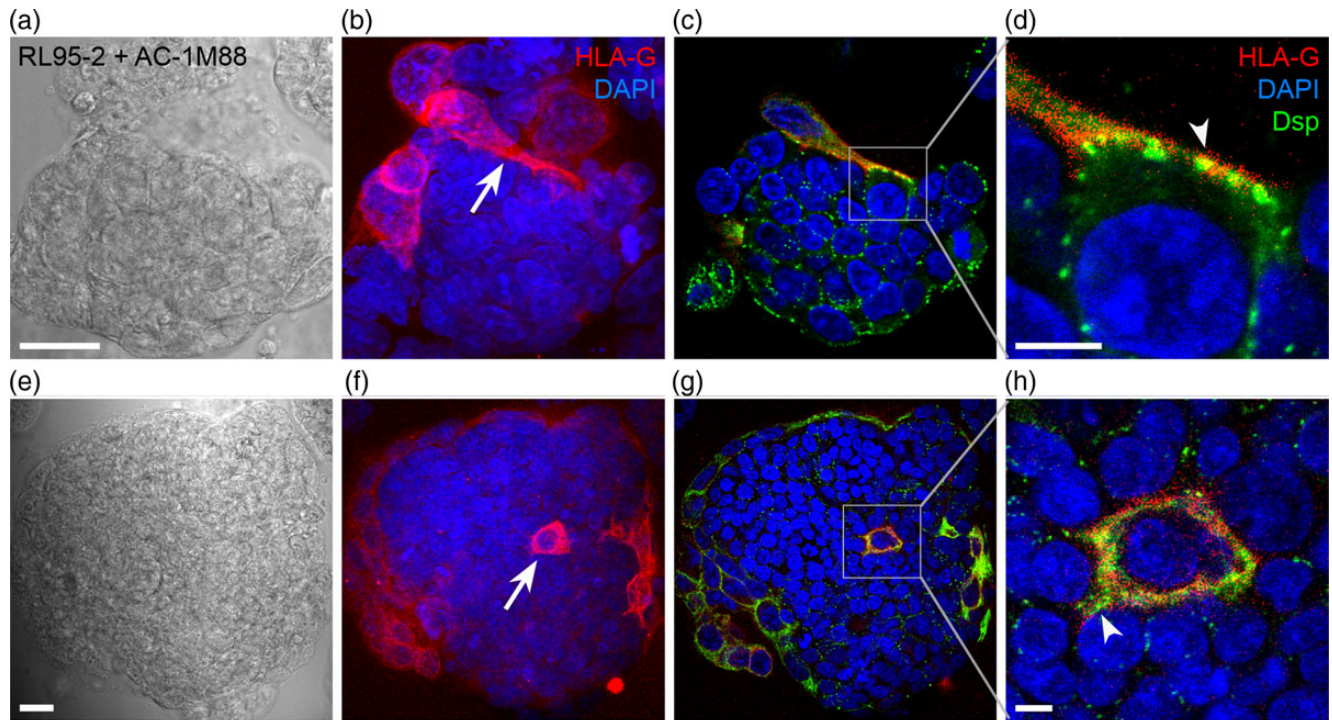


**Figure 6** Desmosomal contacts at human trophoblast-endometrial confrontation sites in 3D. Two confrontation sites of RL95-2 spheroids with AC-1M88 trophoblast cells after 9 days in Matrigel™ and 5 days after addition of trophoblast cells are shown. DIC micrographs of single confocal planes of the confrontation sites are presented in (a) and (e). Recording of trophoblast-specific HLA-G fluorescence (red) and staining of nuclei (DAPI, blue) were combined in z-stack projections of eight consecutive confocal planes to illustrate the topography of the confrontation sites and the morphology of the invading AC-1M88 cells (arrows in b and f). Additionally, Dsp (green stain) is shown in single confocal planes (c and g) and at higher magnification (d and h). Desmosomal cell–cell contacts between invading trophoblast cells and EECs were clearly identified in high resolution confocal scans (arrowheads in d and h). Scale bars for (a–c) and (e–g) represent 20 μm. Scale bars in (d) and (h) represent 5 μm.

confronted with primary EECs (Bentin-Ley *et al.*, 2000). In that study, desmosomal contact sites were observed between trophoblast cells and EECs by electron microscopy.

Taken together the observations on human tissues and primary material led to the hypothesis that endometrial glands prepare for trophoblast invasion by changes in glandular EEC polarity. The data in the current study provide strong experimental evidence for this notion. To confirm the hypothesis that the epithelium has to become more permissive during the implantation window and that this is correlated with a less polarized epithelium we have performed experiments with differently polarized endometrial cell lines representing the non-receptive proliferative phase of the endometrial epithelium (HEC-1-A) and the receptive secretory phase (RL95-2). Our new model system is set up to mimic implantation and invasion events occurring in the *in vivo* situation in endometrial glands. In contrast to experiments focusing on the very first apical adhesion and attachment of the blastocyst during early embryo implantation we now investigate invasion of EVT's into and through intact gland-like structures.

The idea of endometrial gland invasion by trophoblast cells is closely related to the function assigned to endometrial glands during early implantation and the first trimester. Before the hemotrophic supply of the embryo is fully established during the first trimester of pregnancy, uterine glands provide histiotrophic nutrition for the early conceptus

(Burton *et al.*, 2002). Breaching of the glandular endometrial epithelial barrier by trophoblast cells has been deduced from images of human implantation sites. Images of human implantation (Carnegie Collection; by courtesy of Prof. A.C. Enders; <http://www.trophoblast.cam.ac.uk/info/enders.shtml>) revealed that the trophoblast has invaded underlying endometrial glands through the basement membrane of the uterine epithelium in places at stage 5A, i.e. as early as 1 day after the initiation of implantation. Also in later stages EVT cells cross the glandular basement membrane from basal to apical as shown by Moser *et al.* (2010). In that study on first trimester explant confrontation cultures 'endoglandular trophoblast' cells were found to replace glandular epithelial cells indicating that this alternative route of invasion represents a mechanism to open uterine glands for histiotrophic nutrition of the embryo (Fitzgerald *et al.*, 2010). Based on these findings our study was focused on interactions between invasive EVT cells and glandular EECs.

As a model for single invasive trophoblast cells we chose the fusion cell line AC-1M88, which is of EVT cell origin and shows a migratory capacity as determined by transwell migration assays (Gellersen *et al.*, 2013). The differently polarized and differentiated EEC lines that were cultured in the 3D matrix served as a model for glandular epithelium with different grades of polarity and differentiation (Hannan *et al.*, 2010). Recently, Chitcholtan *et al.* (2013) performed spheroid formation assays with EEC lines in Matrigel™ to investigate aspects of differentiation. Corroborating

our findings in the 3D culture setting, they also observed differences in lumen formation in spheroids of Ishikawa versus RL95-2 cells.

Many studies have been performed to investigate the very early attachment of the blastocyst to the apical luminal epithelium of the endometrium. The advantage of the new model system described in our study is the experimental 3D approach to investigate trophoblast invasion into endometrial glandular structures, which occurs at a later stage of implantation and placentation and might be very important for successful establishment of pregnancy in the first trimester.

In conclusion, we have shown that maternal epithelial junction distribution and polarity affects the degree of trophoblast invasiveness, which is a prerequisite for successful implantation. Less differentiated and polarized EECs facilitate the invasion of EVT cells, while strongly polarized EECs are not invaded. Considering the importance of adequate endometrial differentiation, further studies are planned with primary endometrial cells of patients undergoing IVF treatment. We expect that the newly established 3D confrontation culture system will provide new insights in early implantation events and contribute to the improvement of success rates in assisted reproductive technology.

## Supplementary data

Supplementary data are available at <http://humrep.oxfordjournals.org/>.

## Acknowledgements

We acknowledge the advice of Prof. Klaus Ebnet and Hüseyin Tuncay at the Institute of Medical Biochemistry (ZMBE), Münster University during the development of the spheroid cell culture system. Thanks are due to Sabina Hennes-Mades for her skilful technical assistance in cell culture.

## Authors' roles

V.U.B.: conception and design, experimental work, acquisition of data, analysis and interpretation of data, manuscript writing, final approval of the manuscript. B.G.: participation in study design, critical discussion and final approval of the manuscript. R.E.L.: participation in study design, critical discussion and revision and final approval of the manuscript. I.C.-L.: conception and design, analysis and interpretation of data, manuscript writing, critical revision and final approval of the manuscript.

## Funding

This work was supported by Grant I46/14, 'START-Program', Medical Faculty, RWTH Aachen University, to V.U.B., by Grant Lec\_16\_12, 'RWTH Lecturer Award', RWTH Aachen University to I.C.-L. and by the German Research Council (Grant LE 566-20-1).

## Conflict of interest

The authors declare no conflict of interest.

## References

Bentin-Ley U, Horn T, Sjogren A, Sorensen S, Falck Larsen J, Hamberger L. Ultrastructure of human blastocyst-endometrial interactions *in vitro*. *J Reprod Fertil* 2000;**120**:337–350.

Buck VU, Windoffer R, Leube RE, Classen-Linke I. Redistribution of adhering junctions in human endometrial epithelial cells during the implantation window of the menstrual cycle. *Histochem Cell Biol* 2012;**137**:777–790.

Burton GJ, Watson AL, Hempstock J, Skepper JN, Jauniaux E. Uterine glands provide histiotrophic nutrition for the human fetus during the first trimester of pregnancy. *J Clin Endocrinol Metab* 2002;**87**:2954–2959.

Chitcholtan K, Asselin E, Parent S, Sykes PH, Evans JJ. Differences in growth properties of endometrial cancer in three dimensional (3D) culture and 2D cell monolayer. *Exp Cell Res* 2013;**319**:75–87.

Enders AC. Trophoblast-uterine interactions in the first days of implantation: models for the study of implantation events in the human. *Semin Reprod Med* 2000;**18**:255–263.

Fitzgerald JS, Germeyer A, Huppertz B, Jeschke U, Knofler M, Moser G, Scholz C, Sonderegger S, Toth B, Markert UR. Governing the invasive trophoblast: current aspects on intra- and extracellular regulation. *Am J Reprod Immunol* 2010;**63**:492–505.

Funayama H, Gaus G, Ebeling I, Takayama M, Füzesi L, Huppertz B, Kaufmann P, Frank HG. Parent cells for trophoblast hybridization II: AC1 and related trophoblast cell lines, a family of HGPRT-negative mutants of the choriocarcinoma cell line JEG-3. *Placenta* 1997;**18**(Suppl 2):191–201.

Gaus G, Funayama H, Huppertz B, Kaufmann P, Frank H-G. Parent cells for trophoblast hybridization I: Isolation of extravillous trophoblast cells from human term chorion laeve. *Placenta* 1997;**18**(Suppl 2):181–190.

Gellersen B, Reimann K, Samalecos A, Aupers S, Bamberger AM. Invasiveness of human endometrial stromal cells is promoted by decidualization and by trophoblast-derived signals. *Hum Reprod* 2010;**25**:862–873.

Gellersen B, Wolf A, Kruse M, Schwenke M, Bamberger AM. Human endometrial stromal cell-trophoblast interactions: mutual stimulation of chemotactic migration and promigratory roles of cell surface molecules CD82 and CEACAM1. *Biol Reprod* 2013;**88**:80.

Gonzalez M, Neufeld J, Reimann K, Wittmann S, Samalecos A, Wolf A, Bamberger AM, Gellersen B. Expansion of human trophoblastic spheroids is promoted by decidualized endometrial stromal cells and enhanced by heparin-binding epidermal growth factor-like growth factor and interleukin-1 beta. *Mol Hum Reprod* 2011;**17**:421–433.

Grummer R, Hohn HP, Mareel MM, Denker HW. Adhesion and invasion of three human choriocarcinoma cell lines into human endometrium in a three-dimensional organ culture system. *Placenta* 1994;**15**:411–429.

Hannan NJ, Paiva P, Dimitriadis E, Salamonsen LA. Models for study of human embryo implantation: choice of cell lines? *Biol Reprod* 2010;**82**:235–245.

Hohn HP, Denker HW. Experimental modulation of cell-cell adhesion, invasiveness and differentiation in trophoblast cells. *Cells Tissues Organs* 2002;**172**:218–236.

Holmberg JC, Haddad S, Wunsche V, Yang Y, Aldo PB, Gnainsky Y, Granot I, Dekel N, Mor G. An *in vitro* model for the study of human implantation. *Am J Reprod Immunol* 2012;**67**:169–178.

Illingworth IM, Kiszka I, Bagley S, Ireland GW, Garrod DR, Kimber SJ. Desmosomes are reduced in the mouse uterine luminal epithelium during the preimplantation period of pregnancy: a mechanism for facilitation of implantation. *Biol Reprod* 2000;**63**:1764–1773.

Koot YE, Teklenburg G, Salker MS, Brosens JJ, Macklon NS. Molecular aspects of implantation failure. *Biochim Biophys Acta* 2012;**1822**:1943–1950.

Kuramoto H, Hamano M, Imai M. HEC-1 cells. *Hum Cell* 2002;**15**:81–95.

Lee J, Oh JS, Cho C. Impaired expansion of trophoblast spheroids cocultured with endometrial cells overexpressing cellular retinoic acid-binding protein 2. *Fertil Steril* 2011;**95**:2599–2601.

Moser G, Gauster M, Orendi K, Glasner A, Theuerkauf R, Huppertz B. Endoglandular trophoblast, an alternative route of trophoblast invasion? Analysis with novel confrontation co-culture models. *Hum Reprod* 2010;**25**:1127–1136.

Nishida M. The Ishikawa cells from birth to the present. *Hum Cell* 2002;**15**:104–117.

- Preston AM, Lindsay LA, Murphy CR. Desmosomes in uterine epithelial cells decrease at the time of implantation: an ultrastructural and morphometric study. *J Morphol* 2006;**267**:103–108.
- Schlafke S, Enders AC. Cellular basis of interaction between trophoblast and uterus at implantation. *Biol Reprod* 1975;**12**:41–65.
- Schmitz C, Yu L, Bocca S, Anderson S, Cunha-Filho JS, Rhavi BS, Oehninger S. Role for the endometrial epithelial protein MFG-E8 and its receptor integrin  $\alpha v \beta 3$  in human implantation: results of an *in vitro* trophoblast attachment study using established human cell lines. *Fertil Steril* 2014;**101**:874–882.
- Thie M, Denker HW. *In vitro* studies on endometrial adhesiveness for trophoblast: cellular dynamics in uterine epithelial cells. *Cells Tissues Organs* 2002;**172**:237–252.
- Thie M, Fuchs P, Denker HW. Epithelial cell polarity and embryo implantation in mammals. *Int J Dev Biol* 1996;**40**:389–393.
- Thie M, Rospel R, Dettmann W, Benoit M, Ludwig M, Gaub HE, Denker HW. Interactions between trophoblast and uterine epithelium: monitoring of adhesive forces. *Hum Reprod* 1998;**13**:3211–3219.
- Wang H, Pilla F, Anderson S, Martinez-Escribano S, Herrero I, Moreno-Moya JM, Musti S, Bocca S, Oehninger S, Horcajadas JA. A novel model of human implantation: 3D endometrium-like culture system to study attachment of human trophoblast (Jar) cell spheroids. *Mol Hum Reprod* 2012;**18**:33–43.
- Wang H, Bocca S, Anderson S, Yu L, Rhavi BS, Horcajadas J, Oehninger S. Sex steroids regulate epithelial-stromal cell cross talk and trophoblast attachment invasion in a three-dimensional human endometrial culture system. *Tissue Eng Part C Methods* 2013;**19**:676–687.
- Way DL, Grosso DS, Davis JR, Surwit EA, Christian CD. Characterization of a new human endometrial carcinoma (RL95-2) established in tissue culture. *In Vitro* 1983;**19**:147–158.